NUCL SCI TECH (2016) 27:32
DOI 10.1007/s41365-016-0029-2

Investigation on hydrogen absorption/desorption properties of as-cast $La_{(1-x)}Mg_xNi_{4.25}Al_{0.75}$ ($x = 0.0, 0.1, 0.2, 0.3$) alloys for tritium storage

Li-Jun Lü[1,3] · **Hong-Hui Cheng**[1,2] · **Xing-Bo Han**[1] · **Guan-Hong Lei**[1] ·
Wei Liu[1] · **Xiao-Lin Li**[1]

Received: 4 February 2015 / Revised: 10 May 2015 / Accepted: 10 May 2015 / Published online: 6 April 2016

Abstract $La_{(1-x)}Mg_xNi_{4.25}Al_{0.75}$ ($x = 0.0, 0.1, 0.2, 0.3$) alloys for tritium storage were prepared by a method of electromagnetic induction melting. The crystal structure and hydrogen storage performance of the as-cast alloys were investigated. The results showed that a single phase of $LaNi_4Al$ was in the alloys with $x = 0.0$ and 0.1 and that $LaNi_4Al$ and second phase of $(La,Mg)Ni_3$ and $AlNi_3$ were in the alloys with $x = 0.2$ and 0.3. On the other hand, the plateau pressures of P–C isotherms of the alloys were increased with the rise of the x value from 0.2 to 0.3 and the hydrogen storage capacity was obviously degraded simultaneously. It was found that the alloy had faster absorption kinetics as the proportion of Mg increased from 0.1 to 0.3.

Keywords Tritium · RE tritium storage alloy · Mg substitution · Hydrogen storage properties

1 Introduction

Molten FLiNaKBe salt can be used as fuel and heat transfer media in nuclear reactor, due to its advantage of high thermal conductivity, low viscosity and high boiling point, etc. [1, 2]. The research on thorium-based molten salt reactors (TMSR) has been launched in China [3]. However, tritium as a product of fuel fission and neutron absorption by lithium in the salt would be generated when the TMSR is running [4]. Thus, it is necessary to find a safe way to store the tritium for its high mobility and radioactivity [5].

Solid state storage of hydrogen isotopes (H, D and T) in the form of metal hydrides/deuterides/tritides is considered as the safest and the most advantageous method over conventional storage methods like gaseous storage in high-pressure gas cylinders and liquid storage in cryogenic tanks [6, 7]. For the storage of tritium as metal tritides in tritium-handling facilities, it should have low equilibrium pressure, high absorption capacity and delivery of high purity ^3He-free tritium without the use of pumps [8]. As a favored material, $LaNi_{4.25}Al_{0.75}$ alloy was used in tritium-processing facilities to store tritium at the Savannah River Site (SRS) in the USA because it is easily activated, a delivery pressure of >200 kPa is easily achieved by moderate heating, and it captures nearly the entire ^3He [9]. So far, $LaNi_{4.25}Al_{0.75}$ alloy as a tritium storage medium has been used for more than 20 years [8]. Cheng et al. [10] reported the hydrogen storage performance of $LaNi_{4.25}Al_{0.75}/SiO_2$ composite and found that the composite possess excellent pulverization resistance with cycles. The effect of SiO_2 encapsulation on the hydrogen absorption kinetics of $LaNi_{4.25}Al_{0.75}$ in a hydrogen atmosphere with a tiny amount of CO impurity was studied by Han et al. [11].

✉ Hong-Hui Cheng
31834385@qq.com

✉ Xiao-Lin Li
lixl@sinap.ac.cn

[1] Shanghai Institute of Applied Physics, Chinese Academy of Sciences, Jiading Campus, Shanghai 201800, China

[2] College of Mechanical Engineering, Yangzhou University, Yangzhou 225127, China

[3] University of Chinese Academy of Sciences, Beijing 100049, China

Moreover, the effect of hydrogen absorption/desorption cycling on the hydrogen storage performance of $LaNi_{4.25}Al_{0.75}$ was reported by Cheng et al. [12], and it was found that cycling could result in pulverization of the bulk alloy.

Mg- and Mg–Ni-based alloys, which have a low cost, have been used for onboard hydrogen storage recently due to their rather high hydrogen storage capacity [13, 14]. Besides, the Mg-based hydrides possess good quality functional properties, such as heat resistance, reversibility and recyclability [15]. Hence, a partial substitution of Mg for La in $LaNi_{4.25}Al_{0.75}$ alloys may improve tritium storage properties of the alloy. Moreover, it would be more economical in manufacturing because metal Mg is much cheaper than metal La. However, information about the substitution of Mg for La in $LaNi_{4.25}Al_{0.75}$ alloys is scarce. Thus, it is necessary to investigate the tritium absorption/desorption properties of $La_{(1-x)}Mg_xNi_{4.25}Al_{0.75}$ alloys. Tritium is a radioactive gas. Most experiments related to development of tritium storage materials are primarily carried out using hydrogen and deuterium. Owing to the similar chemical properties, reactions of hydrogen isotopes with alloys form their corresponding hydrides, deuterides and tritides with same stoichiometry [16]. As an alternative to tritium, therefore, hydrogen was used to study the tritium storage properties of as-cast $La_{(1-x)}Mg_xNi_{4.25}Al_{0.75}$ alloys in this study.

2 Experimental section

The as-cast $La_{(1-x)}Mg_xNi_{4.25}Al_{0.75}$ alloys ($x = 0.0$, 0.1, 0.2, 0.3) used in this study were prepared by an electromagnetic induction melting furnace with a cold crucible at Metallurgical Laboratory of Shanghai University. The purities of the starting materials were 99.5, 99.9, 99.99 and 99.95 % for La, Ni, Al and Mg, respectively. The melting was carried out under argon atmosphere. Because the saturated vapor pressure of magnesium is significantly high, a three-step melting method was used to reduce the loss of Mg. First, the $La_{(1-x)}Ni_{4.25}Al_{0.75}$ alloy was prepared with Al, La and Ni placed in the crucible from bottom to top. The as-cast ingot of the $La_{(1-x)}Ni_{4.25}Al_{0.75}$ alloy was mechanically crushed to pieces after the preparation. Second, Mg was put into the bottom of the crucible and covered with the $La_{(1-x)}Ni_{4.25}Al_{0.75}$ pieces to melt the $La_{(1-x)}Mg_xNi_{4.25}Al_{0.75}$ alloy. Finally, the as-cast ingot of $La_{(1-x)}Mg_xNi_{4.25}Al_{0.75}$ alloy was broken into pieces and melted again under the same conditions to get a homogeneous alloy. Some magnesium was lost in the melting procedure. In this work, thus, a 15 % excess of Mg was added in the melting to offset the loss.

The crystal structure of the alloys was measured by an X-ray diffractometer (XRD, Bruker, D8 ADVANCE type, Germany) at the XRD Laboratory of Nuclear Materials and Engineering Department in Shanghai Institute of Applied Physics, Chinese Academy of Sciences. The X-ray diffractometer worked with the X-ray of Cu Kα and scanned in the 2θ range of 10°–90° at room temperature. The scanning step size and dwell times per step were 0.02° and 0.5 s, respectively. All the alloy samples were mechanically crushed and grinded into powders for the XRD analysis. The Rietveld refinement of the XRD profiles was performed by the TOPAS software to obtain phase abundance and lattice parameters.

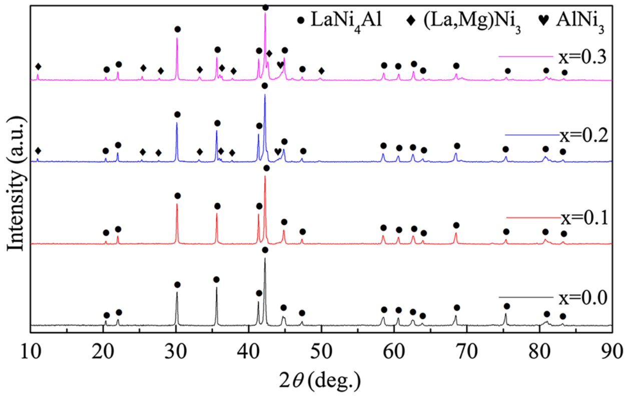

Fig. 1 X-ray diffraction patterns of the $La_{(1-x)}Mg_xNi_{4.25}Al_{0.75}$ alloys

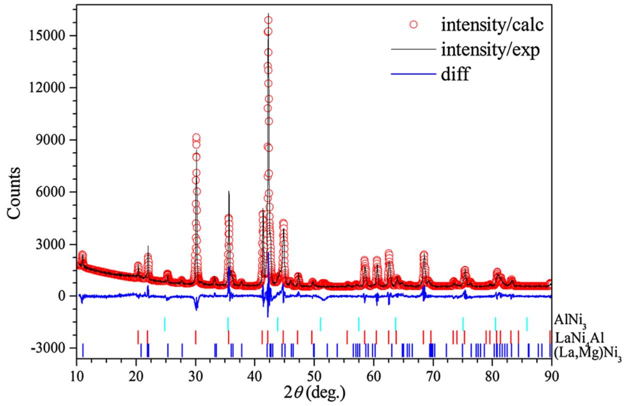

Fig. 2 Rietveld refinement of the observed XRD pattern for the alloy with $x = 0.2$

The hydrogen absorption/desorption pressure-composition isotherms (PCI) of the alloys were measured on a Sieverts apparatus with 99.999 % purity hydrogen gas at the New Energy Material & Technology Laboratory of Yangzhou University. The PCI was obtained by the volumetric technique [17, 18]. The volumetric method is an indirect measurement. It consists of expanding gas from a high-pressure cell into a low-pressure cell during an isothermal process. Hydrogen concentration in alloys can be formulated according to the real-time monitored

Table 1 Lattice constants and phase abundances of the $La_{(1-x)}Mg_xNi_{4.25}Al_{0.75}$ alloys

Alloys	Phases	Space groups	*a* (Å)	*c* (Å)	*V* (Å^3)	Abundance (wt%)
$LaNi_{4.25}Al_{0.75}$	$LaNi_4Al$	P6/mmm	5.0475	4.0449	89.24	100.00
$R_{wp} = 10.26$ %, $S = 2.99$						
$La_{0.9}Mg_{0.1}Ni_{4.25}Al_{0.75}$	$LaNi_4Al$	P6/mmm	5.0428	4.0477	89.14	100.00
$R_{wp} = 9.58$ %, $S = 2.09$						
$La_{0.8}Mg_{0.2}Ni_{4.25}Al_{0.75}$	$LaNi_4Al$	P6/mmm	5.0420	4.0478	89.04	75.28
$R_{wp} = 8.77$ %, $S = 1.91$	$AlNi_3$	Pm$\bar{3}$m	3.5430	–	44.47	9.20
	$(La,Mg)Ni_3$	R$\bar{3}$m	4.9956	24.229	523.66	15.51
$La_{0.7}Mg_{0.3}Ni_{4.25}Al_{0.75}$	$LaNi_4Al$	P6/mmm	5.0367	4.0439	88.84	65.25
$R_{wp} = 10.02$ %, $S = 2.22$	$AlNi_3$	Pm$\bar{3}$m	3.5300	–	43.96	11.65
	$(La,Mg)Ni_3$	R$\bar{3}$m	4.9844	24.170	520.04	23.1

R_{wp} = weighted pattern factor, S = goodness of fit

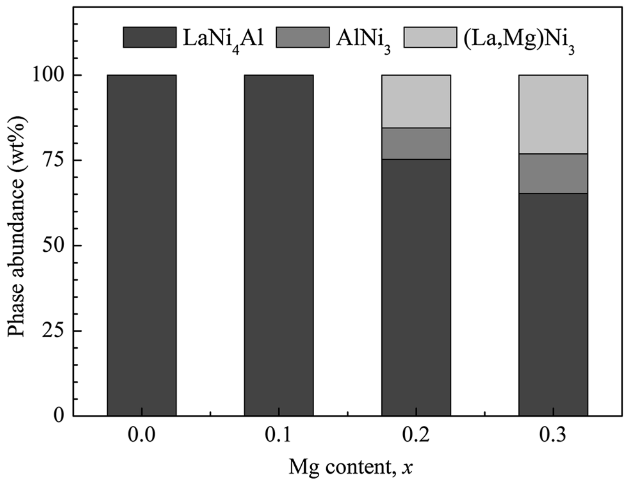

Fig. 3 Phase abundances versus Mg content in the alloys

pressure and temperature, calibrated volumes of different parts, as well as the real equation of state for hydrogen. The kinetics of absorption can be studied by charging high pressure (above the equilibrium value), then recording the drop in the pressure versus time. Desorption can be studied by evacuating to low pressure (below the equilibrium value), then recording the rise in the pressure versus time. Roughly one sample of 1 g was put into the reaction chamber, evacuated at 373 K for 30 min and then reacted with 9 MPa hydrogen gas. After 10 absorption/desorption cycles, the amount of hydrogen absorbed by the sample remained constant. Hence, the alloy was considered to be fully activated. Subsequently, the P–C isotherms of the hydrogen absorption/desorption and absorption kinetics curves were measured at 363, 383 and 403 K, respectively. The research showed that the uncertainty of the PCI measurement was less than 2 % [18]. More detail about the PCI measurement principle, setup and uncertainty can be found in the relevant literature [15, 16].

3 Results and discussion

3.1 Alloy phases and crystal structure

There were three phases in the as-cast $La_{(1-x)}Mg_xNi_{4.25}Al_{0.75}$ ($x = 0.0, 0.1, 0.2, 0.3$) alloys, which were the $LaNi_4Al$ phase [19] with a $CaCu_5$-type hexagonal structure, the $(La,Mg)Ni_3$ phase [20] with a $PuNi_3$-type rhombohedral structure and the $AlNi_3$ phase [21] with a $AuCu_3$-type cubic structure (Fig. 1). The $LaNi_4Al$ and $(La,Mg)Ni_3$ are hydrogen absorbable phases, while the $AlNi_3$ is not such a phase [22, 23]. The Rietveld refinement pattern of the XRD profile for the quantitative phase analysis of the alloy with $x = 0.2$ is represented in Fig. 2, which showed that the calculated patterns by the Rietveld method were in good agreement with the experimental patterns. In the Rietveld refinement, the structure models for the $LaNi_4Al$, $(La,Mg)Ni_3$ and $AlNi_3$ phases were taken from the reported $CaCu_5$ [24], $PuNi_3$ [20] and $AuCu_3$ [21] structures, respectively. Lattice constants and phase abundances are tabulated in Table 1. The values of the Rietveld fit parameters R_{wp} and S are about 10 % and 2, respectively, which indicates the Rietveld refinement and quantitative analysis are reliable in this work (Table 1). The evolution of phase abundance versus Mg content is shown in Fig. 3. It was apparent that the phase structures and abundances of the alloys were varied with Mg contents. When the values of x were 0.0 and 0.1, $LaNi_4Al$ was the only phase to be found in the alloys, suggesting that Mg dissolved into the alloy with $x = 0.1$. As x values increased to 0.2 and 0.3, $(La,Mg)Ni_3$ and $AlNi_3$ phases occurred in the alloys. When the x value increased from 0.2 to 0.3, the abundance of the $LaNi_4Al$ phase

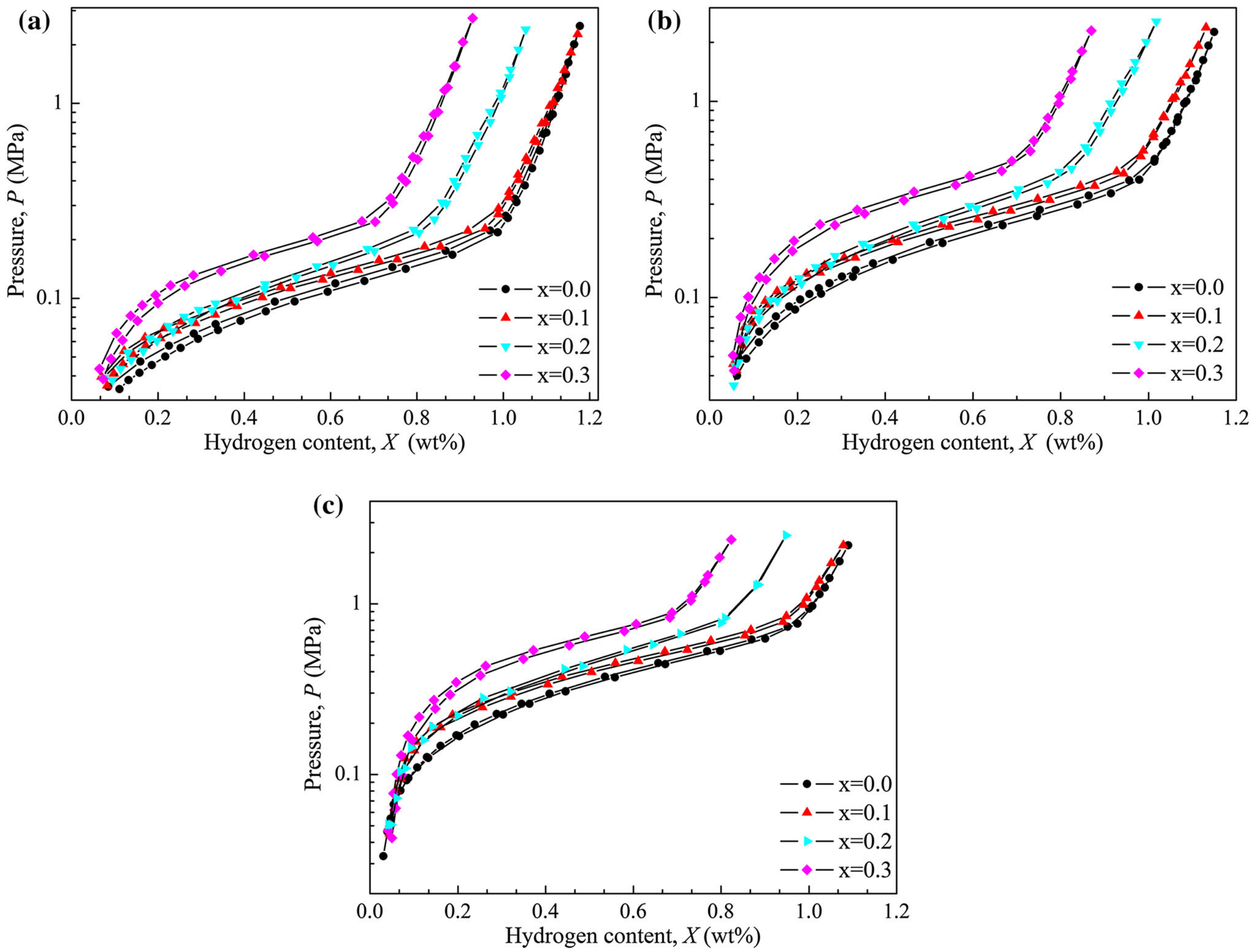

Fig. 4 Absorption/desorption P–C isotherms of the $La_{(1-x)}Mg_xNi_{4.25}Al_{0.75}$ alloys, **a** 363 K; **b** 383 K; **c** 403 K

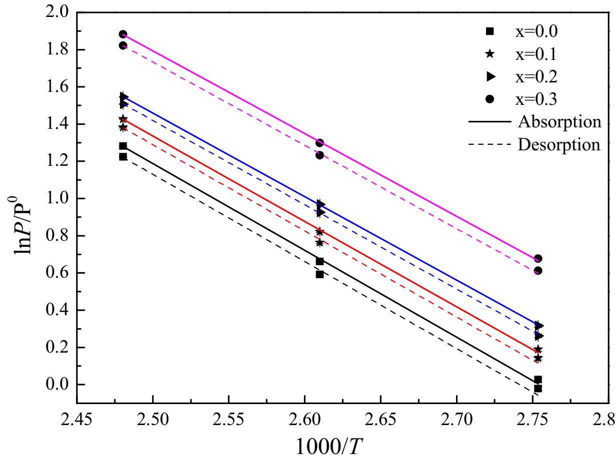

Fig. 5 The van't Hoff curves of $La_{(1-x)}Mg_xNi_{4.25}Al_{0.75}$-H system

fell from 75.28 to 65.25 wt%, whereas the abundances of the $AlNi_3$ and $(La,Mg)Ni_3$ phases increased from 9.20 and 15.51 wt% to 11.65 and 23.1 wt%, respectively. The hydriding/dehydriding properties of the alloys might be affected by these changes of phase abundances.

The crystallographic parameters of every phase in the alloys were in agreement with the published data [25, 26] (Table 1). The cell volumes of the main phase, $LaNi_4Al$, decreased with the increasing Mg content. Likewise, the cell volume of the $(La,Mg)Ni_3$ phase decreased in the alloys with $x = 0.2$ and $x = 0.3$. These might be mainly due to the substitutions of Mg for La. The atomic radii of Mg (1.602 Å) are shorter than La (1.897 Å) [22].

3.2 Pressure-composition isotherms

The hydrogen absorption and desorption P–C isotherms of the as-cast $La_{(1-x)}Mg_xNi_{4.25}Al_{0.75}$ ($x = 0.0$, 0.1, 0.2, 0.3) alloys are shown in Fig. 4. For each alloy, the upper and lower curves are absorption and desorption isotherms, respectively. It can be seen that all the alloys showed one sloping plateau and no significant hysteresis loops between the absorption and desorption curves. Research has shown

Table 2 The thermodynamic properties of $La_{(1-x)}Mg_xNi_{4.25}Al_{0.75}$ alloys

Alloys	ΔH (KJ/mol)		ΔS (J/mol K)		ΔG (KJ/mol) (363 K)		wt% (H)		
	Absorption	Desorption	Absorption	Desorption	Absorption	Desorption	363 K	383 K	403 K
$LaNi_{4.25}Al_{0.75}$	−38.18 ± 0.23	39.00 ± 0.09	−105.9	107.6	0.27	−0.05	1.18	1.15	1.09
$La_{0.9}Mg_{0.1}Ni_{4.25}Al_{0.75}$	−37.99 ± 0.19	38.56 ± 0.21	−106.9	107.9	0.82	−0.63	1.17	1.13	1.08
$La_{0.8}Mg_{0.2}Ni_{4.25}Al_{0.75}$	−37.98 ± 0.18	37.80 ± 0.19	−107.3	106.3	0.96	−0.78	1.05	1.02	0.95
$La_{0.7}Mg_{0.3}Ni_{4.25}Al_{0.75}$	−37.77 ± 0.14	37.76 ± 0.15	−108.9	108.3	1.74	−1.55	0.93	0.87	0.82

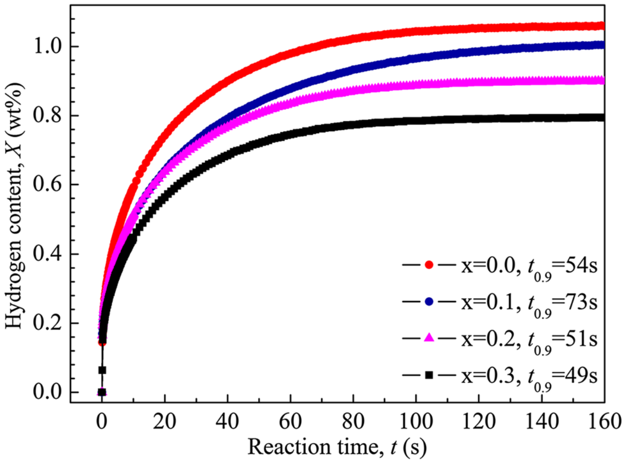

Fig. 6 Hydrogen absorption kinetics of the $La_{(1-x)}Mg_xNi_{4.25}Al_{0.75}$ alloys at 363 K

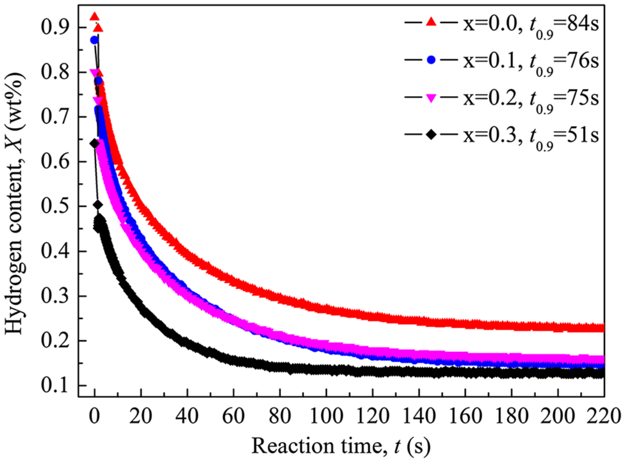

Fig. 7 Hydrogen desorption kinetics of the $La_{(1-x)}Mg_xNi_{4.25}Al_{0.75}$ alloys at 443 K

that the hydrogen absorption/desorption P–C isotherms of an annealed $LaNi_{4.25}Al_{0.75}$ alloy had a flat plateau because the alloy became more homogeneous after anneal treatment [13, 17]. Thus, heat treatment may raise the homogeneity of the $La_{(1-x)}Mg_xNi_{4.25}Al_{0.75}$ ($x = 0.0, 0.1, 0.2, 0.3$) alloys, thereby improving the plateau pressures of their hydrogen absorption/desorption P–C isotherms.

With the elevation of Mg from 0.0 to 0.3, the hydrogen storage capacity decreased from 1.18 to 0.93 wt% and 1.15 to 0.87 wt% at 363 and 383 K, respectively (Fig. 4). Usually, the hydrogen storage capacity would be geometrically connected to the free interstitial space [27]. In this work, the unit cell volume of the hydrogen absorption phases $LaNi_4Al$ and $(La,Mg)Ni_3$ decreased with increasing the Mg content (Table 1), which would lead to a smaller interstitial space to store less hydrogen. In the meantime, the quantitative phase analysis showed that the phase abundance of the $AlNi_3$ phase increased from 9.20 to 11.65 wt% as the x value was raised from 0.2 to 0.3 (Table 1). The $AlNi_3$ is not a hydrogen absorbable phase. The formation enthalpy was low so that it was easy to generate and it was very stable as well [28, 29]. Thus, the increment of the $AlNi_3$ phase abundance in the alloys was the main reason for the degradation of the hydrogen storage capacity.

On the other hand, the addition of Mg resulted in the increment of the absorption/desorption pressure. This indicated that the stability of the alloy hydrides decreased as the Mg increased in the alloys, because the increment of the plateau pressure could be regarded as a measure of the stability for the alloy–hydrogen system [30]. The property might relate to the decrement of the unit cell volume of $LaNi_4Al$ and $(La,Mg)Ni_3$ phases in the alloys (Table 1), because a smaller the unit cell and the interstitial hole size would cause a larger strain energy produced by hydrogen atoms occupying the interstitial site [31]·

3.3 Thermodynamic properties

The enthalpies ΔH and entropies ΔS of the hydrogenation/dehydrogenation of $La_{(1-x)}Mg_xNi_{4.25}Al_{0.75}$ alloys were calculated by the van't Hoff equation:

$$\ln\left(\frac{p_{H_2}}{p_0}\right) = \frac{\Delta H}{RT} - \frac{\Delta S}{R}, \tag{1}$$

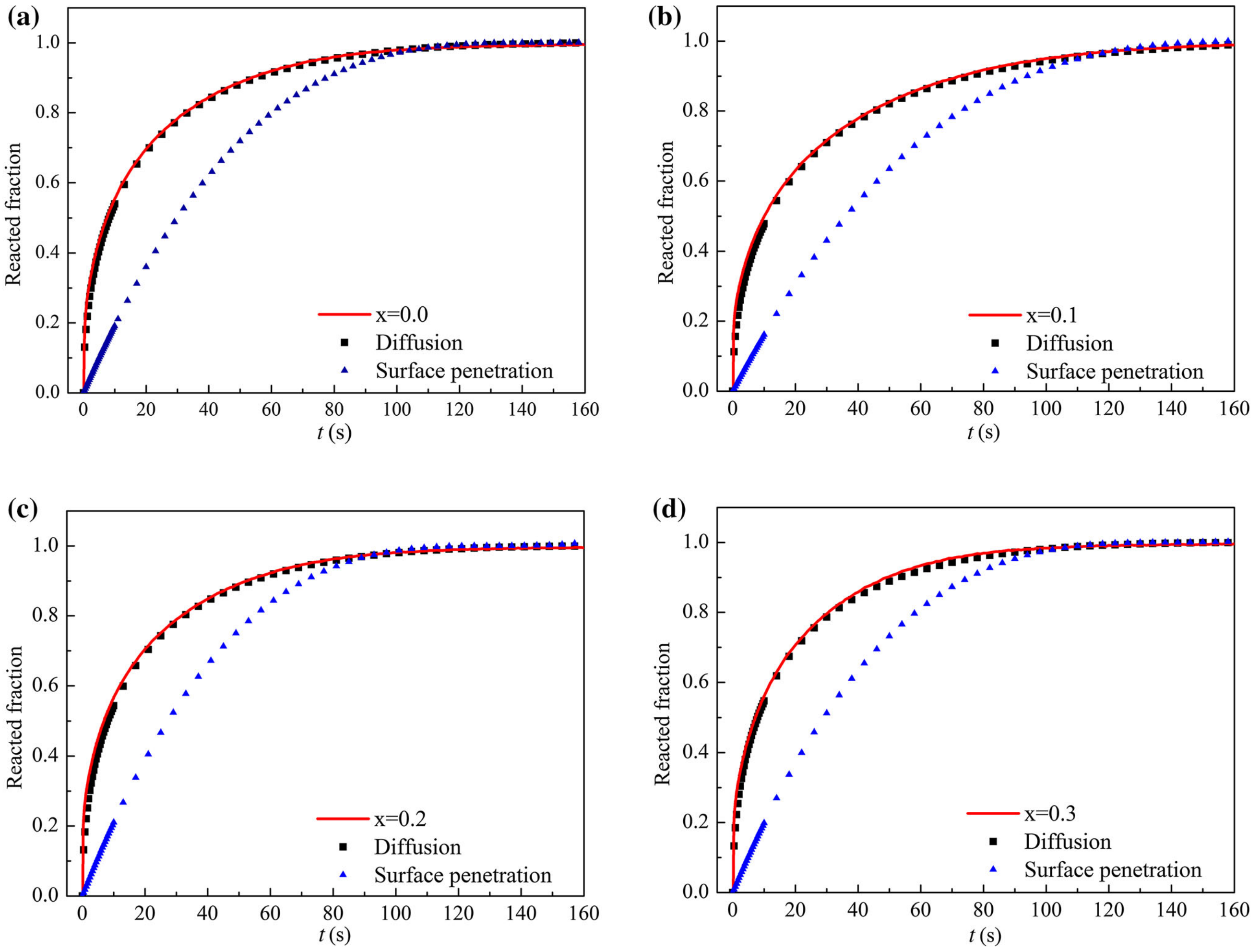

Fig. 8 Hydrogen absorption kinetics of the $La_{(1-x)}Mg_xNi_{4.25}Al_{0.75}$ alloys together with fitting curves of diffusion and surface penetration parts, **a** $x = 0.0$, **b** $x = 0.1$, **c** $x = 0.2$ and **d** $x = 0.3$

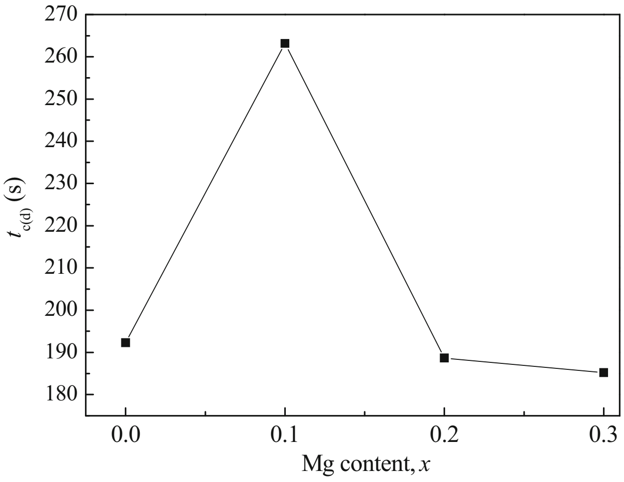

Fig. 9 Characteristic time of diffusion versus Mg content in $La_{(1-x)}Mg_xNi_{4.25}Al_{0.75}$ alloys

where p_{H_2}, T and R are the equilibrium hydrogen gas pressure, the sample temperature and the universal gas constant, respectively. The Gibbs free energy ΔG was calculated according to the following equation:

$$\Delta G = \Delta H - T\Delta S. \tag{2}$$

There were good linear relationships between $\ln p_{H_2}$ and $1/T$ for the as-cast $La_{(1-x)}Mg_xNi_{4.25}Al_{0.75}$ alloys (Fig. 5). The calculation results of the thermodynamics are shown in Table 2. It is obvious that the difference among the absolute enthalpy values of the alloys is not significant with increasing Mg content. The negative value of absorption Gibbs free energy (ΔG_a) confirmed that the stable hydrides were formed in the $La_{(1-x)}Mg_xNi_{4.25}Al_{0.75}$ alloys and decreased with increasing Mg content, because the hydrogen absorption reaction was spontaneous in the direction of decreasing Gibbs free energy [32].

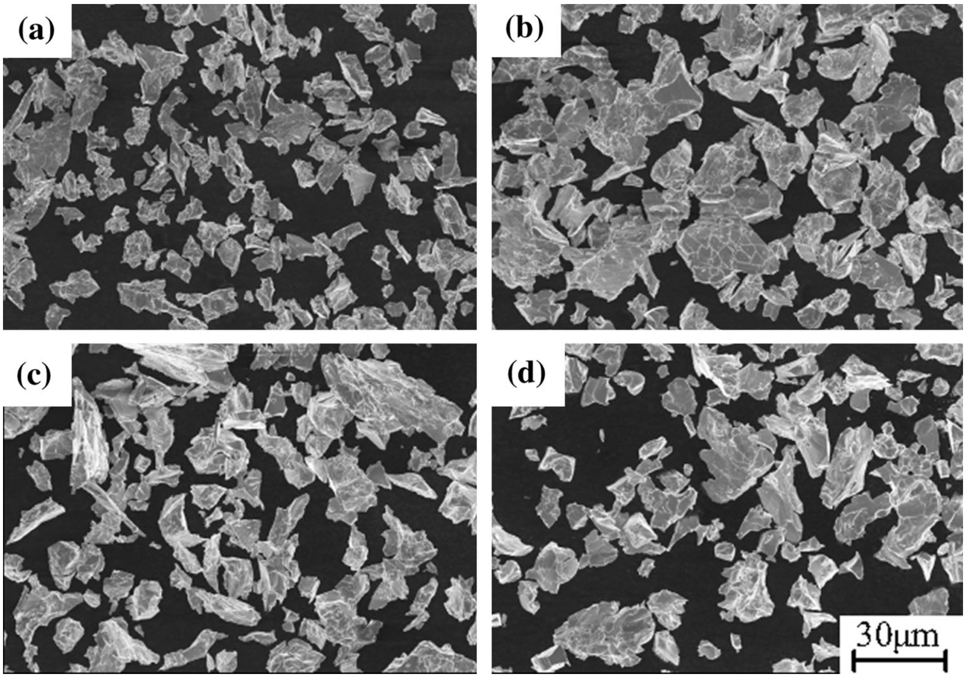

Fig. 10 SEM images of the alloys after 15 absorption/desorption cycles, **a** $LaNi_{4.25}Al_{0.75}$; **b** $La_{0.9}Mg_{0.1}Ni_{4.25}Al_{0.75}$; **c** $La_{0.8}Mg_{0.2}Ni_{4.25}Al_{0.75}$ and **d** $La_{0.7}Mg_{0.3}Ni_{4.25}Al_{0.75}$

3.4 Hydrogen absorption/desorption kinetics

The hydrogen absorption and desorption kinetics of the $La_{(1-x)}Mg_xNi_{4.25}Al_{0.75}$ alloys were assessed in this work. Because the reaction time is relative to the hydrogen absorption capacity of an alloy, the reaction time taken for absorbing/desorbing 90 % of the maximum hydrogen ($t_{0.9}$) is usually used to evaluate the hydrogen absorption/desorbing kinetics of alloys. The $t_{0.9}$ values of the alloys with $x = 0.0$, 0.1, 0.2 and 0.3 for absorption kinetics were 54, 73, 51 and 49 s (Fig. 6), respectively, and for desorption kinetics were 84, 76, 75 and 51 s, respectively (Fig. 7). The results indicated that the absorption/desorption kinetics of the alloys became faster with the increase of Mg content from 0.1 to 0.3.

The model fitting method is widely used to investigate hydrogen absorption kinetics of AB_5-type hydrogen storage alloys. The rate-limiting step was divided into diffusion and surface penetration parts for the Chou model [33, 34]. For the diffusion, the relationship between the fraction (ξ) and time (t) can be illustrated as:

$$\xi = 1-\left(1-\sqrt{\frac{t}{t_{c(d)}}}\right)^3. \tag{3}$$

When the rate-controlling step is the surface penetration, the essential rate can be expressed as:

$$\xi = 1-\left(1-\frac{t}{t_{c(sp)}}\right)^3, \tag{4}$$

$t_{c(d)}$ is proportional to R_0^2 and $t_{c(sp)}$ is proportional to R_0, where R_0 is the radius of the particles [35].

In this work, Eqs. (3) and (4) were used to fit the hydrogen absorption kinetics (Fig. 8). It was obvious that the fitting lines calculated from the diffusion model showed a better agreement with the experimental data of the alloys. Thus, the diffusion was the rate-controlling step. The calculated results of $t_{c(d)}$ are shown in Fig. 9. It was shown that the alloy with $x = 0.1$ had the maximum value of $t_{c(d)}$, which result in the biggest particle size R_0. In order to investigate the powdered features of the alloys, the morphology of the alloys after 15 hydrogen absorption/desorption cycles was observed by a scanning electron microscope (SEM, Fig. 10). It can be found that the particles of the alloys were not uniform after the absorption/desorption cycles. This was due to the volume expansion from hydrogen absorption and volume shrinkage from hydrogen desorption. For AB_5-type alloy, the higher the c/a ratio is, the bigger the particle size is [36]. In addition, the less the hydrogen storage capability of the alloy is, which would result in a smaller volume expansion in the absorption of hydrogen is, the bigger the particle size is. The particle size increased with an increase in Mg content when $x = 0.0$ and 0.1, but decreased when $x = 0.2$ and 0.3, which was in accordance with the variation of $t_{c(d)}$. The biggest particle size was the reason for a slow hydrogen absorption kinetic when $x = 0.1$.

4 Conclusion

Presently, there is no information on the substitution of Mg for La in $LaNi_{4.25}Al_{0.75}$ alloys. Thus, this research is focused on potentional tritium storage performance of as-cast $La_{(1-x)}Mg_xNi_{4.25}Al_{0.75}$ alloys. Some conclusions obtained from the research were as follows:

1. The as-cast $La_{(1-x)}Mg_xNi_{4.25}Al_{0.75}$ alloys showed a single phase with $CaCu_5$-type structure when $x = 0.0$ and 0.1. However, for $x = 0.2$ and 0.3, second phases with $PuNi_3$-type and $AuCu_3$-type structures occurred in the alloys, and the abundance of the second phase increased with the rise of the x value.
2. With the addition of Mg, the plateau pressure of the alloys increased and their hydrogen storage capacity decreased. The degradation of the hydrogen storage capacity was mainly caused by the increment of $AlNi_3$ phase abundance.
3. The rate-controlling step for the alloys was diffusion. With the increment of Mg content from 0.1 to 0.3, the absorption kinetics of the alloys became faster. The results implied that it is beneficial to develop new tritium storage alloys with good kinetics.

Acknowledgments This work was financially supported by the Strategic Priority Research Program of the Chinese Academy of Sciences (XDA02020200), the National Natural Science Foundation of China (No. 11475145) and the Yangzhou Foundation for Development of Science and Technology (No. YZ2014041). The authors are grateful to Prof. Yun-Bo Zhong and Ph.D. student Li-Jun Fan at the Metallurgical Laboratory of Shanghai University for the alloy melting.

References

1. J. Qiu, Y. Zou, G.J. Yu et al., Compatibility of container materials with Cr in molten Flinak salt. J. Fluor. Chem. **168**, 69–74 (2014). doi:10.1016/j.jfluchem.2014.09.010
2. W.G. Liu, H. Han, C.L. Ren et al., The effect of Nb additive on Te-induced stress corrosion cracking in Ni alloy: a first-principles calculation. Nucl. Sci. Tech. **25**, 050603 (2014). doi:10.13538/j.1001-8042/nst.25.050603
3. X. Zhou, G. Liu, Study of control rod worth in the TMSR. Nucl. Sci. Tech. **1**, 010601 (2013). doi:10.13538/j.1001-8042/nst.2013.01.003
4. Y.S. Zeng, S.W. Wu, Y. Qian et al., Apparatus for determining permeability of hydrogen isotopes in molten-salt. Nucl. Sci. Tech. **25**, 040602 (2014). doi:10.13538/j.1001-8042/nst.25.040602
5. X.S. Zhou, G.J. Chen, S.M. Peng et al., Thermal desorption of tritium and helium in aged titanium tritide films. Int. J. Hydrogen Energy **39**, 11006–11015 (2014). doi:10.1016/j.ijhydene.2014.05.102
6. F. Mannone, *Safety in Tritium Handling Technology* (Springer, The Netherlands, 1993), p. 236
7. D. Pukazhselvan, V. Kumar, S.K. Singh, High capacity hydrogen storage: basic aspects, new developments and milestones. Nano Energy. **1**, 566–589 (2012). doi:10.1016/j.nanoen.2012.05.004
8. W.D. Wang, X.G. Long, G.J. Cheng et al., Tritium absorption–desorption characteristics of $LaNi_{4.25}Al_{0.75}$. J. Alloys Compd. **441**, 359–363 (2007). doi:10.1016/j.jallcom.2006.09.122
9. K.L. Shanahan, J.S. Hölder, D.R. Bell et al., Tritium aging effects in $LaNi_{4.25}Al_{0.75}$. J. Alloys Compd. **356–357**, 382–385 (2003). doi:10.1016/S0925-8388(03)0139-7
10. H.H. Cheng, H.G. Yang, S.L. Li et al., Hydrogen storage performance of $LaNi_{4.25}Al_{0.75}/SiO_2$ composite. Rare Metal Mater. Eng. **37**, 1427–1430 (2008). **(in Chinese)**
11. X.B. Han, H.G. Yang, W. Chen et al., Effect of SiO_2 encapsulation on hydrogen absorption kinetics of $LaNi_{4.25}Al_{0.75}$ in hydrogen atmosphere with tiny amount of CO impurity. Rare Metal Mater. Eng. **42**, 2525–2529 (2013). **(in Chinese)**
12. H.H. Cheng, H.G. Yang, S.L. Li et al., Effect of hydrogen absorption/desorption cycling on hydrogen storage performance of $LaNi_{4.25}Al_{0.75}$. J. Alloys Compd. **453**, 448–452 (2008). doi:10.1016/j.jallcom.2006.11.112
13. W. Grochala, P.P. Edwards, Thermal decomposition of the non-interstitial hydrides for the storage and production of hydrogen. Chem. Rev. **104**, 1283–1316 (2004). doi:10.1021/cr030691s
14. M. Zhu, H. Wang, L.Z. Ouyang et al., Composite structure and hydrogen storage properties in Mg-base alloys. Int. J. Hydrogen Energy **31**, 251–257 (2006). doi:10.1016/j.ijhydene.2005.04.030
15. B. Sakintuna, F. Lamari-Darkrim, M. Hirscher, Metal hydride materials for solid hydrogen storage: a review. Int. J. Hydrogen Energy **32**, 1121–1140 (2007). doi:10.1016/j.ijhydene.2006.11.022
16. R.A. Jat, S.C. Parida, R. Agarwal et al., Investigation of hydrogen isotope effect on storage properties of Zr–Co–Ni alloys. Int. J. Hydrogen Energy **39**, 14868–14873 (2014). doi:10.1016/j.ijhydene.2014.07.045
17. H.H. Cheng, W.B. Li, W. Chen et al., Development of hydrogen absorption–desorption experimental test bench for hydrogen storage material. Int. J. Hydrogen Energy **39**, 13596–13602 (2014). doi:10.1016/j.ijhydene.2014.03.015
18. H.H. Cheng, X.X. Deng, S.L. Li et al., Design of PC based high pressure hydrogen absorption/desorption apparatus. Int. J. Hydrogen Energy **32**, 3046–3053 (2007). doi:10.1016/j.ijhydene.2007.01.010
19. T. Takeshita, S.K. Malik, W.E. Wallace, Hydrogen absorption in RNi_4Al (R = rare earth) ternary compounds. J. Solid State Chem. **23**, 271–274 (1978). doi:10.1016/0022-4596(78)90074-9
20. K. Kadir, T. Sakai, I. Uehara, Synthesis and structure determination of a new series of hydrogen storage alloys; RMg_2Ni_9 (R = La, Ce, Pr, Nd, Sm and Gd) built from $MgNi_2$ laves-type layers alternating with AB_5 layers. J. Alloys Compd. **257**, 115–121 (1997). doi:10.1016/S0925-8388(96)03132-5
21. P.V.M. Rao, S.V. Suryanarayana, K.S. Murthy et al., The high-temperature thermal expansion of Ni_3Al measured by X-ray diffraction and dilation methods. J. Phys. Condens. Matter **1**, 5357–5361 (1989). doi:10.1088/0953-8984/1/32/004
22. R.V. Denys, V.A. Yartys, Effect of magnesium on the crystal structure and thermodynamics of the $La_{3-x}Mg_xNi_9$ hydrides. J. Alloys Compd. **509**, S540–S548 (2011). doi:10.1016/j.jallcom.2010.11.205
23. R.J. Zhang, M.Q. Lu, D.L. Cao et al., Effect of Al content on hydrogen storage capacity and plateau pressure of $LaNi_{5-x}Al_x$–H system. Chin. J. Rare Metals **28**, 678–682 (2004). doi:10.13373/j.cnki.cjrm.2004.04.017. **(in Chinese)**
24. H. Nakamura, Y. Nakamura, S. Fujitani et al., A method for designing a hydrogen absorbing $LaNi_{5-x-y}Mn_xAl_y$ alloy for a chemical refrigeration system. J. Alloys Compd. **252**, 83–87 (1997). doi:10.1016/S0925-8388(96)02611-4
25. D.L. Cao, D.M. Chen, Y. Liu et al., Structure and hydrogen storage performance of $LaNi_{4.25}Al_{0.75}$ alloy. Trans. Nonferr. Metal Soc. China **21**, 517–522 (2011). doi:10.1016/S1003-6326(11)60745-0
26. B. Liao, Y.Q. Lei, G.L. Lu et al., The electrochemical properties of $La_xMg_{3-x}Ni_9$ ($x = 1.0$–2.0) hydrogen storage alloys. J. Alloys Compd. **356**, 746–749 (2003). doi:10.1016/S0925-8388(03)00083-5
27. H. Ye, H. Zhang, J.X. Cheng et al., Effect of Ni content on the structure, thermodynamic and electrochemical properties of the

non-stoichiometric hydrogen storage alloys. J. Alloys Compd. **308**, 163–171 (2000). doi:10.1016/S0925-8388(00)01049-5

28. H.H. Cheng, *Special hydrogen storage materials and the measurement apparatus*. Ph.D. Thesis, Institute of Metal Research, Chinese Academy of Sciences, 2007, pp. 51–52
29. D.M. Shi, B. Wen, R. Melnik et al., First-principles studies of Al–Ni intermetallic compounds. J. Solid State Chem. **182**, 2664–2669 (2009). doi:10.1016/j.jssc.2009.07.026
30. S.L. Li, P. Wang, W. Chen et al., Study on hydrogen storage properties of $LaNi_{3.8}Al_{1.2-x}Mn_x$ alloys. Int. J. Hydrogen Energy **35**, 12391–12397 (2010). doi:10.1016/j.ijhydene.2010.08.049
31. S.L. Li, P. Wang, W. Chen et al., Effect of non-stoichiometry on hydrogen storage properties of $La(Ni_{3.8}Al_{1.0}Mn_{0.2})_x$ alloys. Int. J. Hydrogen Energy **35**, 3537–3545 (2010). doi:10.1016/j.ijhydene.2010.01.102
32. S.L. Li, P. Wang, W. Chen et al., Hydrogen storage properties of $LaNi_{3.8}Al_{1.0}M_{0.2}$ (M = Ni, Cu, Fe, Al, Cr, Mn) alloys. J. Alloys Compd. **485**, 867–871 (2009). doi:10.1016/j.jallcom.2009.06.111
33. K.C. Chou, A kinetic model for oxidation of Si–Al–O–N materials. J. Am. Ceram. Soc. **89**, 1568–1576 (2006). doi:10.1111/j.1551-2916.2006.00959.x
34. K.C. Chou, K.D. Xu, A new model for hydriding and dehydriding reactions in intermetallics. Intermetallics **15**, 767–777 (2007). doi:10.1016/j.intermet.2006.10.004
35. X.H. An, Y.B. Pan, Q. Luo et al., Application of a new kinetic model for the hydriding kinetics of $LaNi_{5-x}Al_x$ ($0 \leq x \leq 1.0$) alloys. J. Alloys Compd. **506**, 63–69 (2010). doi:10.1016/j.jallcom.2010.07.016
36. Y.H. Zhang, X.L. Wang, M.Y. Chen et al., Design of chemical compositions on AB_5-type hydrogen storage alloy with high quality. Met. Funct. Mater. **9**, 1–6 (2002). **(in Chinese)**